

Resonant spin-dependent electron coupling in a III-V/II-VI heterovalent double quantum well

A. A. Toropov, I. V. Sedova, S. V. Sorokin, Ya. V. Terent'ev, E. L. Ivchenko, and S. V. Ivanov
Ioffe Physico-Technical Institute, Russian Academy of Sciences, St. Petersburg 194021, Russia

We report on design, fabrication, and magneto-optical studies of a III-V/II-VI hybrid structure containing a GaAs/AlGaAs/ZnSe/ZnCdMnSe double quantum well (QW). The structure design allows one to tune the QW levels into the resonance, thus facilitating penetration of the electron wave function from the diluted magnetic semiconductor ZnCdMnSe QW into the nonmagnetic GaAs QW and vice versa. Magneto-photoluminescence studies demonstrate level anticrossing and strong intermixing resulting in a drastic renormalization of the electron effective g factor, in perfect agreement with the energy level calculations.

PACS numbers: 75.70.Cn, 78.67.Pt, 75.50.Pp, 85.75.Mm

The great majority of currently used semiconductor device heterostructures are *isovalent*, i.e., they involve compounds of the same chemical group. The design and fabrication of *heterovalent* heterostructures, including compounds of different groups, are hampered because of the lack of precise data on the properties and technology of heterovalent interfaces. Particularly discouraging are the presence of polarization charges at the interface and poor technological reproducibility of such basic interface properties as band offsets etc. On the other hand, certain useful characteristics of the heterovalent structures are unachievable in the isovalent ones. One known example is the reduced holes leakage in mid-infrared optoelectronic devices based on InAs, due to the realization of a huge valence band offset at an InAs/CdSe interface.¹

Another opportunity can be a flexible engineering of magneto-electronic and magneto-optical properties in a III-V/II-VI hybrid structure involving a high-quality III-V part, e.g., a GaAs/AlGaAs quantum well (QW), and a diluted magnetic semiconductor (DMS) II-VI part, e.g. a ZnCdMnSe/ZnSe QW. Such structures can combine large solubility of magnetic ions in the II-VI DMS² and high electron mobilities as well as long electron spin relaxation times in a non-magnetic III-V part.³ This combination can be useful for both fundamental studies of spin-polarized two-dimensional electron gas and device applications in the rapidly growing field of spintronics.

In this paper we report on the realization of a double QW structure, where a GaAs/AlGaAs QW is electronically coupled with a DMS ZnCdMnSe/ZnSe QW through a heterovalent AlGaAs/ZnSe interface. We show that the proper structure design allows one to achieve resonant tunnelling conditions, which facilitates extension of the electron wave function in the II-VI DMS region, resulting in giant values of the effective g factor in both the GaAs-like and ZnCdMnSe-like electronic states.

The sample design and principles of operation are illustrated in Fig. 1. Figure 1a shows schematically the conduction band line-ups of the structure. The QW parameters are chosen in such a way that at zero magnetic field the lowest confined electron level in the ZnCdMnSe QW is nearly resonant with the lowest electron level in

the GaAs QW. The calculated squared envelope wave function of the lowest-energy electron state in the coupled QWs at zero magnetic field is plotted in Fig. 1b (solid curve). The electron probability is almost equally distributed between the two QWs. The primary effect of a relatively low external magnetic field applied in the Faraday geometry is a giant Zeeman splitting in the DMS QW, caused by the exchange interaction between electrons and Mn^{2+} ions.² As a result, the magnetic field removes spin degeneracy, pushing the electron level with spin component $s = -1/2$ down and the level $s = +1/2$ up. Due to the splitting, the interwell coupling strength is different for the electrons with different spin orientations. The spin asymmetry is well seen in Fig. 1b showing the ground state electron wave functions for $s = \pm 1/2$ at the magnetic field $B = 4.5$ T. The calculation is performed by using the envelope function approach as well as the mean-field approximation while describing Brillouin-like paramagnetic behavior of the Mn^{2+} ions.²

The calculated electron levels versus magnetic field are

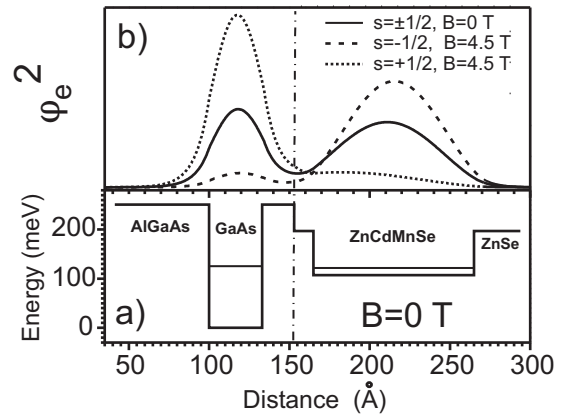


FIG. 1: (a) Conduction band line-ups of the double QW sample. Geometrical parameters correspond to the experimental sample with the 3.4 nm wide GaAs QW. (b) Spin-up (dotted curve) and spin-down (dashed curve) squared electron wave functions calculated for the magnetic field 4.5 T. Solid curve shows the zero-field wave function.

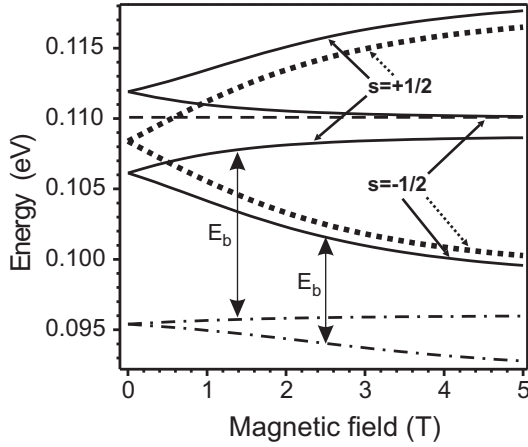


FIG. 2: Electron level variation with the magnetic field in the double QW structure. The structure parameters are the same as in Fig. 1. Dashed and dotted curves represent the levels in isolated GaAs and ZnCdMnSe QWs, respectively. Solid curves show the four levels in the coupled QWs, while a pair of dash-and-dotted curves show the lowest spin-up and spin-down electron levels with subtracted exciton binding energies.

shown in Fig. 2. The diamagnetic shift of the levels as well as the Zeeman level splitting due to the intrinsic g factors are neglected since they are weak as compared with the effect of exchange interaction with the magnetic ions. The dashed and dotted curves in Fig. 2 illustrate the variation of energy levels in the corresponding uncoupled single QWs. Within the used approximation the level in the isolated GaAs QW remains spin degenerate (dashed curve). At zero magnetic field, due to the interwell coupling, the levels are repulsed, their splitting increases by a factor of 3, but the double degeneracy is not lifted. At low magnetic field, the spin splitting of each level is linear in B and, due to the strong level mixing, the splittings are comparable. As the field increases, the single-QW levels with $s = 1/2$ first approach each other, merge at $B \approx 0.6$ T and then move apart. This explains a drastic anticrossing of these levels when the interwell coupling is switched on. In contrast, the increasing magnetic field loosens the interwell coupling of the levels with $s = -1/2$. This resonant magnetic-field-induced control of level mixing should manifest itself in magneto-optical spectra not only in a giant splitting between the lowest levels with $s = \pm 1/2$ but also in a remarkable red-shift of their center-of-mass. Penetration of the heavy hole states into the ZnCdMnSe QW is prohibited due to the huge valence band offset at the GaAs/ZnSe interface (~ 1.1 eV) as well as the larger value of the effective mass.

Realization of the proposed design relies on the controlled fabrication of a high-quality interface between the III-V and II-VI parts. The (Al)GaAs/ZnSe interface is at present most studied among other heterovalent interfaces. Its technology was thoroughly developed for the growth of ZnSe-based optoelectronic devices on GaAs substrates.⁴ More recently, injection of

spin-polarized electrons through a GaAs/ZnSe heterointerface has been realized in an (In)GaAs/AlGaAs QW light-emitting diode with a II-VI DMS spin aligner grown on top.^{5,6} Furthermore, photoluminescence was detected from an AlAs/GaAs/ZnSe QW with a heterovalent interface.⁷ However, to the best of our knowledge, the electron resonant tunnelling through a heterovalent interface has not been observed so far.

The samples were grown by molecular-beam epitaxy on GaAs(001), with the III-V and II-VI growth chambers being connected via an ultra-high vacuum transfer module. The GaAs QW sandwiched between $\text{Al}_{0.3}\text{Ga}_{0.7}\text{As}$ barriers was grown at a substrate temperature $T_S = 580\text{--}600^\circ\text{C}$ and an As/Ga flux ratio as low as possible. The top barrier was as thin as 2 nm. It was capped by one monolayer of GaAs to prevent contamination of the Al-GaAs surface in the transfer chamber. The grown Al-GaAs/GaAs QW structure was cooled down with the $(2 \times 4)\text{As}$ reconstruction. Thereafter the structure was transferred to the II-VI chamber where it was heated up to 280°C keeping the $(2 \times 4)\text{As}$ reconstruction unchanged. The II-VI growth was initiated under the surface exposure to Se flux, which immediately changed the surface reconstruction to (1×1) . The ZnSe growth occurred under the $(2 \times 1)\text{Se}$ -stabilized surface conditions. The II-VI part contained a 10-nm-thick $\text{Zn}_{0.85}\text{Cd}_{0.10}\text{Mn}_{0.05}\text{Se}$ QW embedded between 1.2- and 20-nm-thick ZnSe barriers on bottom and top, respectively.

The thickness of the combined AlGaAs/ZnSe barrier between the GaAs and ZnCdMnSe QWs totals 3.2 nm. The AlGaAs layer is inserted in order to move the heterovalent interface with presumably enhanced density of defects aback from the GaAs QW. The ZnSe spacer is needed for proper II-VI growth initiation and for preventing Mn diffusion in the III-V part, since even low content of Mn in III-V compounds damages their optical quality. The total barrier thickness governs the transfer integral between the single-QW electron wave functions and, hence, the strength of the interwell coupling.

A saturation value of the Zeeman splitting for electrons confined within the ZnCdMnSe QW lies in the range of $15\text{--}20$ meV. This means that the zero-field interlevel energy spacing should be preset to within 10 meV. The fulfillment of this requirement is complicated by the drastic dependence of the conduction band offset (CBO) at a GaAs/ZnSe interface on growth conditions. When the interface growth regime changes from Zn-rich to Se-rich, CBO has been found to vary from 100 meV to 600 meV.⁸ We fixed both the interface and the ZnCdMnSe QW growth conditions and grew a set of structures with different widths of the GaAs QW, which was controlled by growth rate calibrations and transmission electron microscopy measurements. Most intriguing results have been obtained on the structure with a 3.4-nm-thick QW.

To study the effects of interwell electronic coupling we measured low-temperature spectra of GaAs QW excitonic photoluminescence (PL) in a magnetic field applied in the Faraday geometry. A 514 nm line of an Ar^+ laser

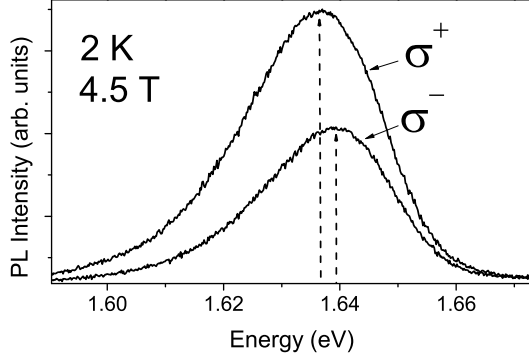


FIG. 3: σ^+ and σ^- polarized PL spectra measured at 4.5 T in the sample with a 3.4 nm wide GaAs QW.

was used as an excitation source. Figure 3 shows the PL spectra of circularly polarized emission components measured in the sample with a 3.4 nm wide GaAs QW at 4.5 T. According to the optical selection rules, the emission components σ^\pm are due to the radiative recombination of the dipole-active excitons $|-1/2, 3/2\rangle$ and $|1/2, -3/2\rangle$, respectively. Here we use the notation $|s, m\rangle$ for an exciton with the electron spin $s = \pm 1/2$ and the hole angular momentum component $m = \pm 3/2$. The PL spectral peaks are split by ~ 3 meV with the lowest-energy peak being σ^+ polarized. The peak energy positions are plotted in Fig. 4 as a function of the magnetic field. These dependencies reflect neither the Zeeman splitting expected for a conventional GaAs/AlGaAs QW nor the symmetrical giant splitting typical for a single DMS QW. Indeed, for a single 3.4 nm GaAs-based QW, the expected spin splitting at 4.5 T would be as small as $0.2 \div 0.3$ meV, taking into account the values $g_e \sim 0.1$ and $g_{hh} \sim -1.6$ for the electron and heavy-hole g factors.⁹ On the other hand, the spin splitting between the $|-1/2, 3/2\rangle$ and $|1/2, -3/2\rangle$ exciton states is quite asymmetric, namely, the exciton level $|1/2, -3/2\rangle$ is rather stable so that the main part of the magnetic-field-induced splitting is con-

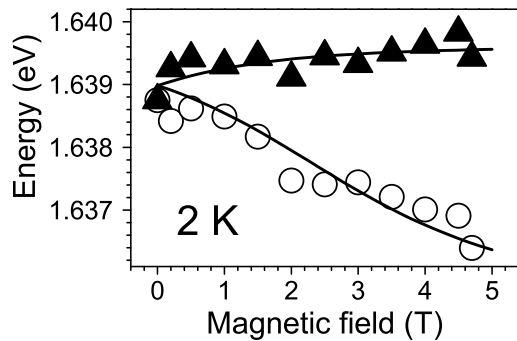


FIG. 4: Energy of the PL peaks corresponding to $|-1/2, 3/2\rangle$ (open circles) and $|1/2, -3/2\rangle$ (solid triangles) excitons. Solid lines represent a theoretical fit (see text).

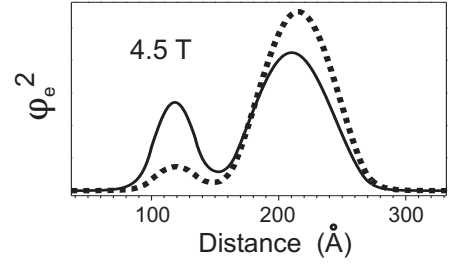


FIG. 5: Electron density $\phi_e^2(z)$ for the spin-down lowest-energy electron state calculated at 4.5 T either neglecting (dotted curve) or taking into account (solid curve) the Coulomb-attraction-induced redistribution of the electron envelope function.

tributed by a red shift of the $|1/2, -3/2\rangle$ exciton level. Therefore we can unambiguously attribute the character of the observed PL band splitting to the effect of resonant coupling between electronic states in the nonmagnetic and DMS QWs. This interpretation is confirmed by the fact that no remarkable splitting has been observed in the off-resonant samples with thicker GaAs QWs, e.g., with a 6-nm-thick QW, where the electronic levels in the nonmagnetic and magnetic QWs are remote far enough.

To describe the experimental data quantitatively, we have calculated the spin-dependent energies of $|1/2, -3/2\rangle$ and $|-1/2, 3/2\rangle$ excitons as a function of magnetic field in the coupled QW system. The band gap of the ZnCdMnSe quaternary solid alloy was interpolated using the known band gap dependence for $\text{Zn}_{1-x}\text{Cd}_x\text{Se}$ ¹⁰ and $\text{Zn}_{1-y}\text{Mn}_y\text{Se}$.¹¹ As regards the ZnCdMnSe/ZnSe interface, we assumed that 75% of the total band offset falls on the conduction band. CBO at the GaAs/ZnSe interface was considered as the only fitting parameter. For the s - d exchange integral and the effective concentration of Mn^{2+} spins, we took the values $N_0\alpha = 0.26$, as in pure ZnMnSe,¹² and 0.03, respectively. The dielectric constant $\epsilon = 11$ was used as an average between those of GaAs ($\epsilon \approx 13$) and ZnSe ($\epsilon \approx 9$).

While calculating the exciton energies we used the self-consistent variational method and chose factorized exciton envelope functions similar to the procedure applied in Ref.¹³. The probe exciton envelope function was taken in the form

$$\Psi = \phi_e(z_e)\phi_h(z_h)f(\rho), \quad (1)$$

where $\phi_e(z)$ and $\phi_h(z)$ are the single-particle electron and hole envelope functions, the envelope function $f(\rho)$ describes the in-plane electron-hole relative motion, z is directed along the growth direction, and ρ denotes the electron-hole in-plane distance. The hole envelope ϕ_h is fixed due to strong confinement in the GaAs QW, its dependence on the magnetic field can be ignored. The electron envelope function is more flexible, and it can be redistributed, as compared with a single-electron state, between the two coupled QWs due to the electron-hole Coulomb attraction. The self-consistent solution of the

coupled Shrödinger equations for the envelopes $\varphi_e(z)$ and $f(\rho)$ was found numerically. The relevance of this approach is illustrated in Fig. 5 showing the shape of φ_e^2 at 4.5 T, calculated either self-consistently or neglecting the Coulomb-attraction-induced redistribution of the electron probability. The Coulomb attraction results in a remarkable increase of probability to find the electron in the GaAs QW. As a consequence, the self-consistent exciton binding energy increases by about 30%.

To compare the theory with the PL experimental data, the Stokes shift adopted as $0.6\Delta_{PL}$, Δ_{PL} being the full width at half maximum of the PL peak,¹⁴ was subtracted from the calculated free-exciton energy. The best theoretical fit obtained in that way is shown in Fig. 4 by solid lines. To illustrate the effect of electron-hole Coulomb interaction on the exciton spin splitting we depicted in Fig. 2, by a pair of dash-and-dotted curves, the spin-up and spin-down lowest-energy electron levels reduced by the self-consistent exciton binding energy. The difference between the curves gives the actual exciton splitting. In agreement with the above analysis the spin-up exciton level is only weakly dependent on the magnetic field. The self-consistent spin-down level approaches, at high magnetic fields, the indirect exciton formed by an electron confined within the ZnCdMnSe QW and a hole confined within the GaAs QW. It is important to stress that, in comparison with the direct (intrawell) exciton, the indirect exciton is characterized by the weaker electron-hole Coulomb interaction and smaller binding energy. The latter effect tends to reduce the exciton spin splitting as compared with the spin splitting of the single-electron levels. In particular, at 4.5 T the exciton spin splitting of 3 meV corresponds to the single-electron spin splitting of 8.8 meV. The difference would be even larger if the calculation did not take into account the Coulomb induced redistribution of electrons and the pronounced difference between the electron effective masses in GaAs

(0.067 m_0) and ZnCdMnSe ($\sim 0.16 m_0$).

The best fit is achieved, assuming the GaAs/ZnSe CBO be equal to 185 meV. This value corresponds to a "mixed" interface, neither Zn- nor Se-rich, in agreement with the short surface exposure to Se at the initial stage of the II-VI growth. This procedure was performed intentionally to bring the QW levels into a resonance in a structure with suitable QW widths. The mixed nature of the interface can also be beneficial for partial elimination of dipole charges at the heterovalent interface, due to averaging the contributions from Zn- and Se-rich microscopic regions having opposite dipole polarities.

In conclusion, we have demonstrated resonant electronic coupling through a heterovalent AlGaAs/ZnSe interface in an optical-quality double QW with the DMS II-VI part. The structure design allows one to resonantly enhance penetration of the nonmagnetic QW electron wave function into the DMS region and enhance the QW electron g factor by more than one order of magnitude. Such structures are especially beneficial for exciton optical studies, since the electron wave function at resonance has a minimum (see the dashed curve in Fig. 1b) at the heterovalent interface with a presumably large density of defects which otherwise could mess up the excitonic properties. Another potential advantage of these hybrid structures is a possibility to insert a similar double QW in a p - i - n or Schottky diode, allowing thus an electric control of the electron spin polarization.

Acknowledgments

This work was supported by the Program of the Ministry of Sciences of RF "Physics of Solid State Nanostructures", INTAS (01-2375), VW Foundation and RFBR (02-02-17643, 03-02-17566). S.V.I. is grateful to RSSF.

- ¹ S. V. Ivanov, V. A. Kaygorodov, S. V. Sorokin, B. Ya. Meltser, V. A. Solovev, Ya. V. Terent'ev, O. G. Lyublinskaya, K. D. Moiseev, E. A. Grebenshchikova, M. P. Mikhailova, A. A. Toropov, Yu. P. Yakovlev, P. S. Kop'ev, and Zh. I. Alferov, Appl. Phys. Lett. **82**, 3782 (2003).
- ² J. K. Furdyna, J. Appl. Phys. **64**, R29 (1988).
- ³ J. M. Kikkawa, I. P. Smorchkova, N. Samarth, and D. D. Awschalom, Science **277**, 1284 (1997).
- ⁴ E. Kato, H. Noguchi, M. Nagai, H. Okuyama, S. Kijima, and A. Ishibashi, Electron. Lett. **34**, 282 (1998).
- ⁵ R. Fiederling, M. Keim, G. Reuscher, W. Ossau, G. Schmidt, A. Waag, and L. W. Molenkamp, Nature **402**, 787 (1999).
- ⁶ B. T. Jonker, Y. D. Park, B. R. Bennett, H. D. Cheong, G. Kioseoglou, and A. Petrou, Phys. Rev. B **62** 8180 (2000).
- ⁷ A. Kudelski, U. Bindley, J. K. Furdyna, M. Dobrowolska, and T. Wojtowicz, Appl. Phys. Lett. **82**, 1854 (2003).
- ⁸ R. Nicolini, L. Vanzetti, G. Mula, G. Bratina,

- L. Sorba, A. Franciosi, M. Peressi, S. Baroni, R. Resta, A. Baldereschi, J. E. Angelo, and W. W. Gerberich, Phys. Rev. Lett. **72**, 294 (1994).
- ⁹ M. J. Snelling, E. Blackwood, C. J. McDonagh, R. T. Harley, and C. T. B. Foxon, Phys. Rev. B **45** 3922 (1992).
- ¹⁰ H. J. Lozykowski, and V. K. Shastri, J. Appl. Phys. **69**, 3235 (1991).
- ¹¹ R. B. Bylsma, W. Becker, J. Kossut, U. Debska, and D. Yoder-Short, Phys. Rev. B **33**, 8207 (1986).
- ¹² A. Twardowski, M. von Ortenberg, M. Demianiuk, and R. Pauthenet, Solid State Commun. **51**, 849 (1984).
- ¹³ E. L. Ivchenko, A. V. Kavokin, V. P. Kochereshko, G. R. Posina, I. N. Uraltsev, D. R. Yakovlev, R. N. Bicknell-Tassius, A. Waag, and G. Landwehr, Phys. Rev. B **46**, 7713 (1992).
- ¹⁴ K. P. O'Donnel, P. J. Parbrook, F. Yang, and C. Trager-Cowan, Physica B **191**, 45 (1993).